The mechanism of linear and nonlinear optical effects in fluoride crystals

Yongzai Tong and X. Y. Meng
Beijing Center for Crystal Research and Development (R&D), Technical Institute of Physics and Chemistry and Graduate School, Chinese Academy of Sciences, P.O. Box 2711, Beijing 100080, China

Z. Z. Wang and Chuangtian Chen[a)]
Beijing Center for Crystal Research and Development (R&D), Technical Institute of Physics and Chemistry, Chinese Academy of Sciences, P.O. Box 2711, Beijing 100080, China

Ming-Hsien Lee
Department of Physics, Tamkang University, Tamsui, Taipei 251, Taiwan

(Received 11 April 2005; accepted 24 May 2005; published online 4 August 2005)

Electronic structure calculations of Na_2SbF_5, $BaMgF_4$, and $BaZnF_4$ are performed from first principles based on a plane-wave pseudopotential method. The linear optical properties and the static second-harmonic generation coefficients are also calculated. Furthermore, a real-space atom-cutting method is employed to analyze the respective contributions of the anionic groups and cations in Na_2SbF_5 to the optical response. The results show that the anionic groups $(SbF_5)^{2-}$ in the crystal are quite favorable for producing larger microscopic second-order susceptibilities. © *2005 American Institute of Physics*. [DOI: 10.1063/1.1977199]

I. INTRODUCTION

With the development of solid-state laser devices, investigations of nonlinear optical (NLO) crystals have become a hotspot of materials science in the past two decades. Scientists have made great efforts to search for new ultraviolet (UV) and deep ultraviolet (DUV) nonlinear optical crystals. Fluoride crystals possess a larger energy gap and an inherently wider transparency region compared with oxide crystals and therefore are suitable for DUV harmonic generation. However, they have in general too small an optical anisotropy (i.e., weak birefringence) to realize phase matching in the UV region and also to have small second-harmonic generation (SHG) coefficients, which is unfavorable for obtaining high-power output at the harmonic frequencies.

To find the special structures of the fluoride crystals that can overcome the above disadvantages it is necessary to study the relationship between their birefringence, SHG coefficients, and microstructures. To our knowledge, CASTEP,[1,2] a plane-wave pseudopotential total-energy package based on density-functional theory (DFT)[3] has been proven to be a useful tool for studying the mechanism of the linear and nonlinear optical effects.

In recent years we have used this theoretical method to calculate the linear refractive indices and SHG coefficients of various NLO crystals such as BBO,[4] LBO,[5] KBBF,[6] SBBO family,[7] KDP,[8] and $SrBe_3O_4$[9] with great success. In this present work we will therefore also use the above method and the CASTEP package to perform *ab initio* calculations of the linear and nonlinear optical coefficients for Na_2SbF_5, $BaMgF_4$, and $BaZnF_4$ and to further explore the mechanism of the optical effects in these crystals. Finally, based on the calculation results and the properties of the strong electronegativity of fluorine atoms in these crystals, future prospects for their application in UV and DUV harmonic generation will be discussed.

II. METHODS AND COMPUTATIONAL DETAILS

The plane-wave pseudopotential total-energy software package CASTEP[1,2] is used for solving the electronic energy-band structures of the fluoride crystals, and these data are further applied to calculate the optical responses. The optimized pseudopotentials[10–12] in the Kleinman-Bylander form for Na, Mg, Zn, Sb, Ba, and F allow us to use a small plane-wave basis set without compromising the accuracy required by our study.

It is well known that the refractive indices can be obtained theoretically from the dielectric function. The imaginary part of the dielectric function can be calculated with the matrix elements which describe the electronic transitions between the ground state and the excited states in the crystal considered. The formula is given by

$$\mathrm{Im}[\varepsilon_{ij}(\omega)] = \frac{e^2}{\pi m^2 h} \sum \int dk \frac{f_{nm} p^i_{nm} p^j_{nm}}{2} \delta_{(\omega_{nm}-\omega)}, \qquad (1)$$

where $f_{nm}=f_n-f_m$ and f_n, f_m are Fermi factors. The real part of the dielectric function is obtained by the Kramers-Kronig transformation.

It is well known that the band gap calculated by the local-density approximation (LDA) is usually smaller than the experimental data due to the discontinuity of exchange-correlation energy. A scissors operator[13,14] is also used to shift upward all the conduction bands in order to agree with measured values of the band gap.

The static limit of the SHG coefficients plays the most important role in the application of SHG crystals. Our group and collaborators have reviewed various calculation methods for SHG coefficients[4,8] and have improved the formula presented by Rashkeev *et al.*[15] to calculate these,

[a)]Electronic mail: cct@cl.cryo.ac.cn

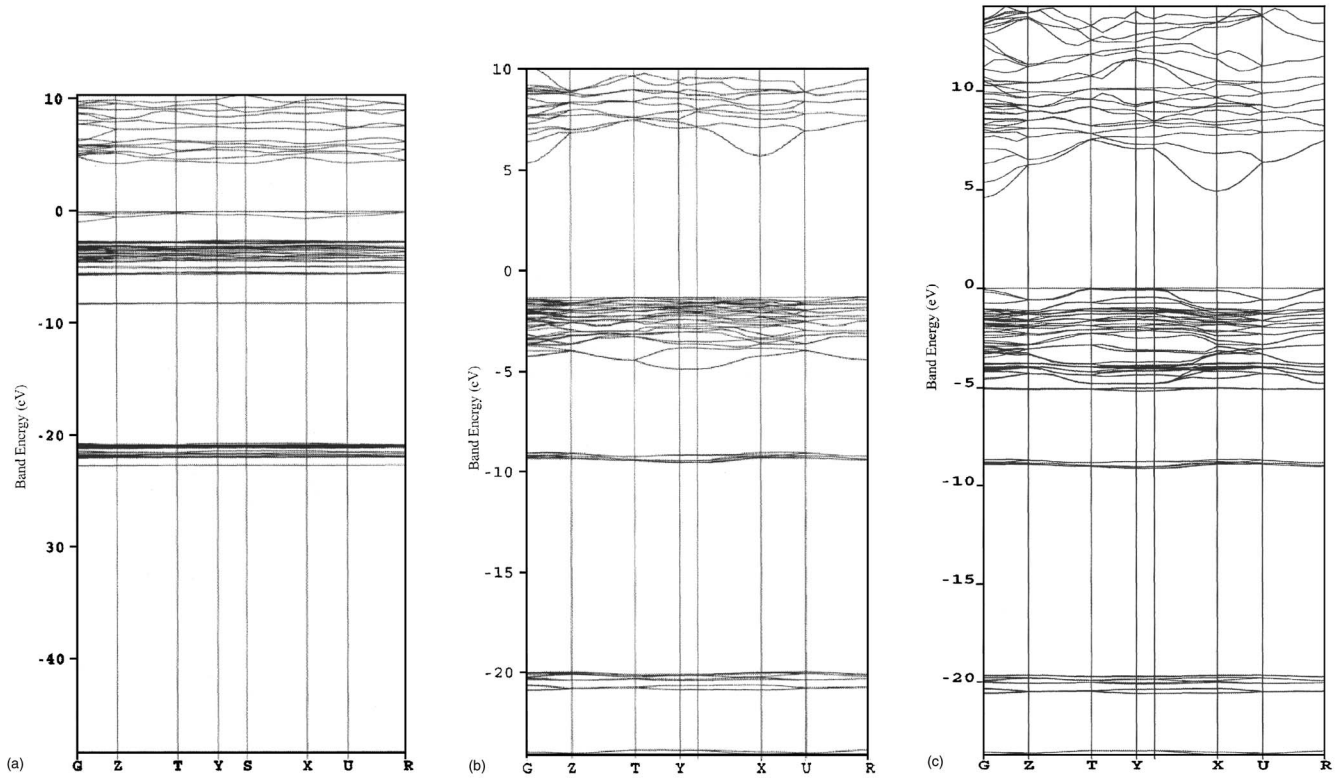

FIG. 1. Band structures of (a) Na_2SbF_5, (b) $BaMgF_4$, and (c) $BaZnF_4$.

$$\chi^{\alpha\beta\gamma} = \chi^{\alpha\beta\gamma}(\mathrm{VE}) + \chi^{\alpha\beta\gamma}(\mathrm{VH}) + \chi^{\alpha\beta\gamma}\ (\text{two bands}), \qquad (2)$$

where $\chi^{\alpha\beta\gamma}(\mathrm{VE})$ and $\chi^{\alpha\beta\gamma}(\mathrm{VH})$ give the contributions to $\chi_i^{(2)}$ from virtual-electron and virtual-hole processes, respectively; $\chi^{\alpha\beta\gamma}(\text{two bands})$ is the contribution to $\chi_i^{(2)}$ from the two-band processes. The formulas for calculating $\chi^{\alpha\beta\gamma}(\mathrm{VE})$, $\chi^{\alpha\beta\gamma}(\mathrm{VH})$, and $\chi^{\alpha\beta\gamma}(\text{two bands})$ are given in Refs. 4 and 8.

To investigate the influence of the ions on the crystal optical response, a real-space atom-cutting method[4] has been used. With this method the contribution of ion A to the nth-order susceptibility denoted as $\chi^{(n)}(A)$ can be obtained by cutting all ions except A from the original wave functions $\chi^{(n)}(A) = \chi^{(\mathrm{n})}$ (all ions except A are cutting).

The Na_2SbF_5, $BaMgF_4$, and $BaZnF_4$ crystals are reported to have structures with $P_{2_12_12_1}$, C_{mc2_1}, and C_{mc2_1} space-group symmetries, respectively. In our calculations we took the cell parameters of Na_2SbF_5, $BaMgF_4$, and $BaZnF_4$ as follows: Na_2SbF_5 ($a = 5.451$ Å, $b = 11.234$ Å, $c = 8.083$ Å, $\alpha = \beta = \gamma = 90°$);[16] $BaMgF_4$ ($a = 4.126$ Å, $b = 14.518$ Å, $c = 5.821$ Å, $\alpha = \beta = \gamma = 90°$); and $BaZnF_4$ ($a = 4.184$ Å, $b = 14.96$ Å, $c = 5.825$ Å, $\alpha = \beta = \gamma = 90°$).[17] These unit cells contain 32, 24, and 24 atoms, respectively.

III. RESULTS AND DISCUSSIONS

A. Band structures

The calculated energy bands of the Na_2SbF_5, $BaMgF_4$, and $BaZnF_4$ crystals are shown in Figs. 1(a), 1(b), and 1(c), respectively. The energy bands are divided into three subgroups: (1) For Na_2SbF_5 in Fig. 1(a) there are an inner region with energies lower than −20 eV, a valence-band region from −10 to 0 eV, and conduction bands above 0 eV. (2) For $BaMgF_4$ in Fig. 1(b) there are an inner region with band energies lower than −15 eV, a valence-band region from −15 to 0 eV, and conduction bands above 0 eV. (3) For $BaZnF_4$ in Fig. 1(c) there are an inner region with energies lower than −10 eV, a valence-band region from −10 to 0 eV, and conduction bands above 0 eV. For the three crystals the calculated gaps are 4.3, 6.7, and 4.66 eV, respectively, to be compared with the experimental ones, 5.0, 9.28, and 7.27 eV. So energy scissors are added to the 0.7, 3.0, and 2.6 eV in order to agree with the experiments.

In order to deeply understand the contributions of the different ions to the optical response, we calculated the total density of state (DOS) and the partial density of state (PDOS) projected on the constitutional atom. The results are shown in Fig. 2. As an example, Figs. 3(a), 3(b), and 3(c) show the orbital-resolved PDOS of Na, Sb, and F in the Na_2SbF_5 crystal, respectively. From the PDOS of Na_2SbF_5, [Fig. 2(a)] the atomic orbitals of sodium atom only contribute to the bottom of the valence band and do nothing to the upper valence band and conduction bands. The 2*s* orbital of Na contributes the peak around −50 eV, and the peak of −22 eV is composed of 2*p* ones. The valence bands are mainly from the mixture of the orbitals of Sb and F atoms. The conduction bands are all composed of the orbitals of Sb and F for which the contributions of Sb are mainly from 5*s* and 5*p* orbitals. The PDOS of $BaMgF_4$ [Fig. 2(b)] shows that the orbitals of Ba only contribute to the bottom of the valence bands and do nothing to the upper valence band and

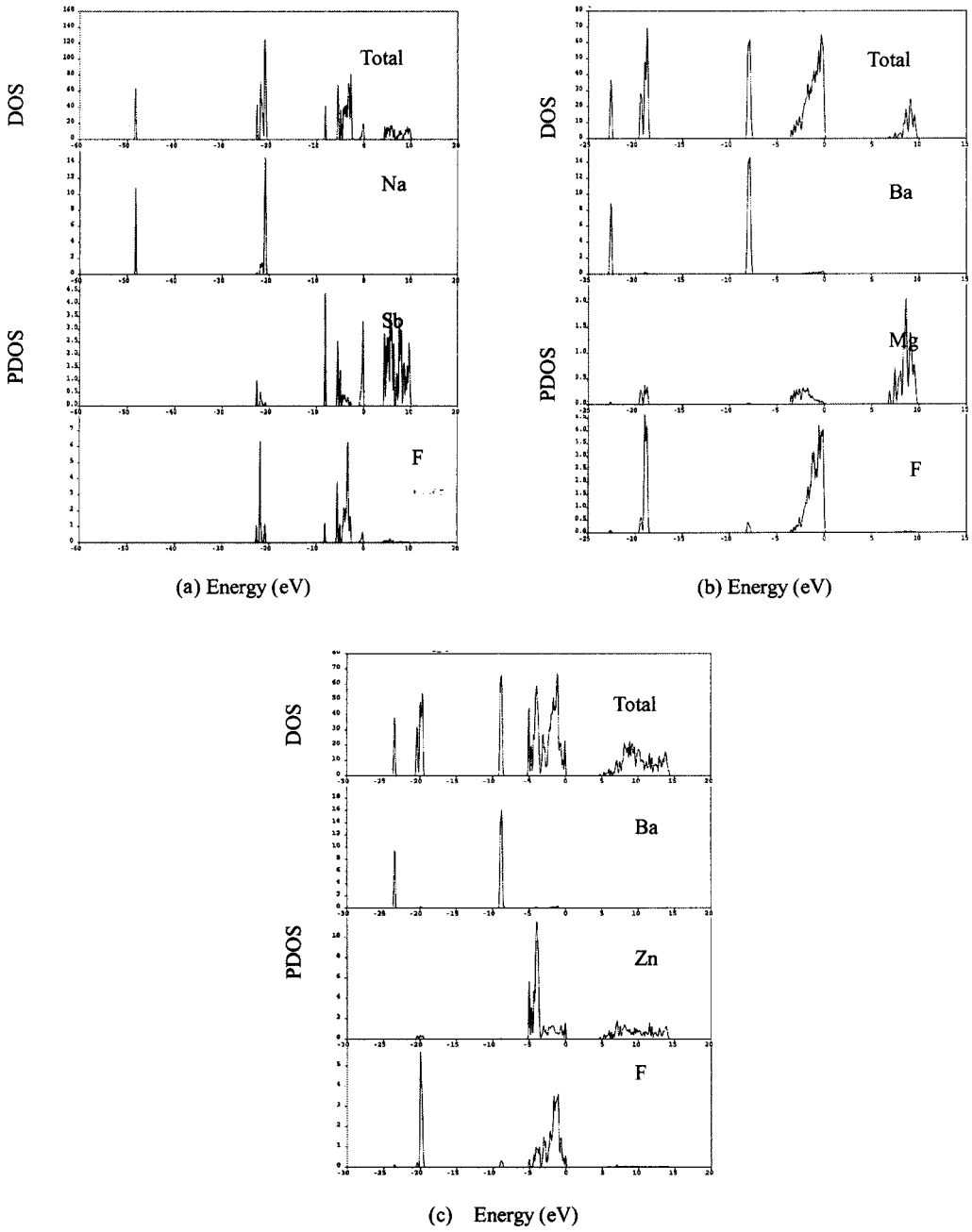

FIG. 2. DOS and PDOS of (a) Na_2SbF_5, (b) $BaMgF_4$, and (c) $BaZnF_4$.

conduction bands. The peak around −23 eV is from the contribution of 5*s* orbitals and the peak of −12 eV is from 5*p* orbitals of Ba. The valence orbitals of the fluorine atom contribute mainly to valence bands for which the peak around −18 eV is from 2*s* and the peak around 0 eV is from 2*p* orbitals. Finally, the conduction bands are mainly composed of 3*s* and 3*p* orbitals of the Mg atom. Because the harmonic generation is mainly from the electron transitions from the upper valence bands to the bottom of the conduction bands, therefore, the essential mechanism of the harmonic generation is the transition of the electrons in $(SbF_5)^{2-}$ and $(MgF_4)^{2-}$ anionic groups.

B. Optical properties

Based on the above energy-band structures, the linear and nonlinear optical coefficients in the Na_2SbF_5, $BaMgF_4$, and $BaZnF_4$ crystals have been already calculated. Due to the discontinuation of the exchange-correlation energy, the energy gaps calculated are all smaller than the experimental ones, and then scissors operators are used to shift up the conduction bands. The calculated linear and nonlinear optical coefficients are listed in Table I. Obviously, the calculated values are all in good agreement with the experimental ones for the three crystals.

To investigate the influence of the ions on the optical responses of Na_2SbF_5, the atom-cutting method is still used. Figure 4 presents the charge-density distributions of the Na_2SbF_5 crystal. Figure 4(a) shows that there is an obvious overlap between the Sb and F electron clouds, but the electron density of Na is isolated. Therefore we treated F and Sb as a whole $(SbF_5)^{2-}$ group and Na as another one. In Fig. 4(a) the charge-density contours of fluorine atoms are differ-

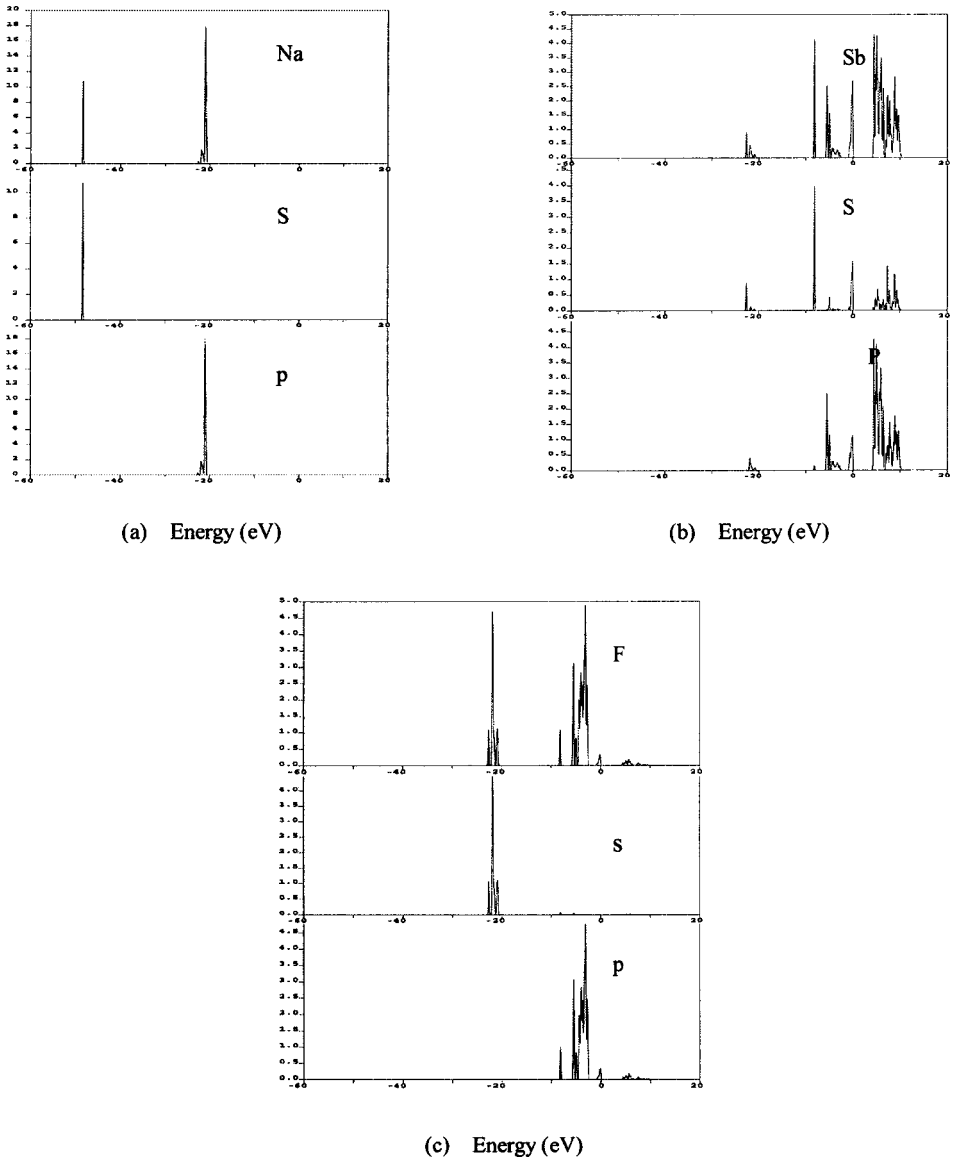

FIG. 3. Orbital-resolved PDOS of Na_2SbF_5 (a) Na, (b) Sb, and (c) F.

ent because all four fluorine atoms cannot stay in the same projecting plane. In our calculation, the radii of Na, Sb, and F are 0.125, 0.100, and 0.107 nm, respectively. When the energy of incidence light is less than the energy gap, the dispersion of SHG coefficients is very small, so it is enough to calculate linear refractive indices and SHG coefficients at zero frequency. In Table II the atom-cutting results are listed for the Na_2SbF_5 crystal. One can easily see from the table that the contribution from Na ion to birefringence is about one-third and the one from the anionic group $(SbF_5)^{2-}$ is

TABLE I. Calculated and experimental values of linear and nonlinear optical coefficients for the Na_2SbF_5, $BaMgF_4$, and $BaZnF_4$ crystals. (Values in parentheses are experimental ones.)

Crystal	Na_2SbF_5 (Ref. 16)	$BaMgF_4$ (Ref. 17)	$BaZnF_4$ (Ref. 17)
Space group	$P_{2_12_12_1}$	C_{mc2_1}	C_{mc2_1}
Energy gap (eV)	4.3 (5.0)	6.7 (9.28)	4.66 (7.27)
Energy scissors (eV)	0.7	3.0	2.6
n_x	1.566 (1.449)	1.462 (1.467)	1.428 (1.514)
n_y	1.573 (1.467)	1.470 (1.439)	1.441 (1.490)
n_z	1.510 (1.462)	1.463 (1.458)	1.432 (1.507)
$\Delta n(n_{\max}-n_{\min})$	0.063 (0.041)	0.008 (0.028)	0.013 (0.024)
d_{jj} (pm/v)	d_{123} -0.154 (0.121)	d_{31} 0.0286 (0.0259)	d_{31} 0.019 (0.009)
		d_{32} 0.0022 (0.0481)	d_{32} 0.033 (0.012)
		d_{33} 0.0828 (0.0185)	d_{33} 0.029 (0.041)

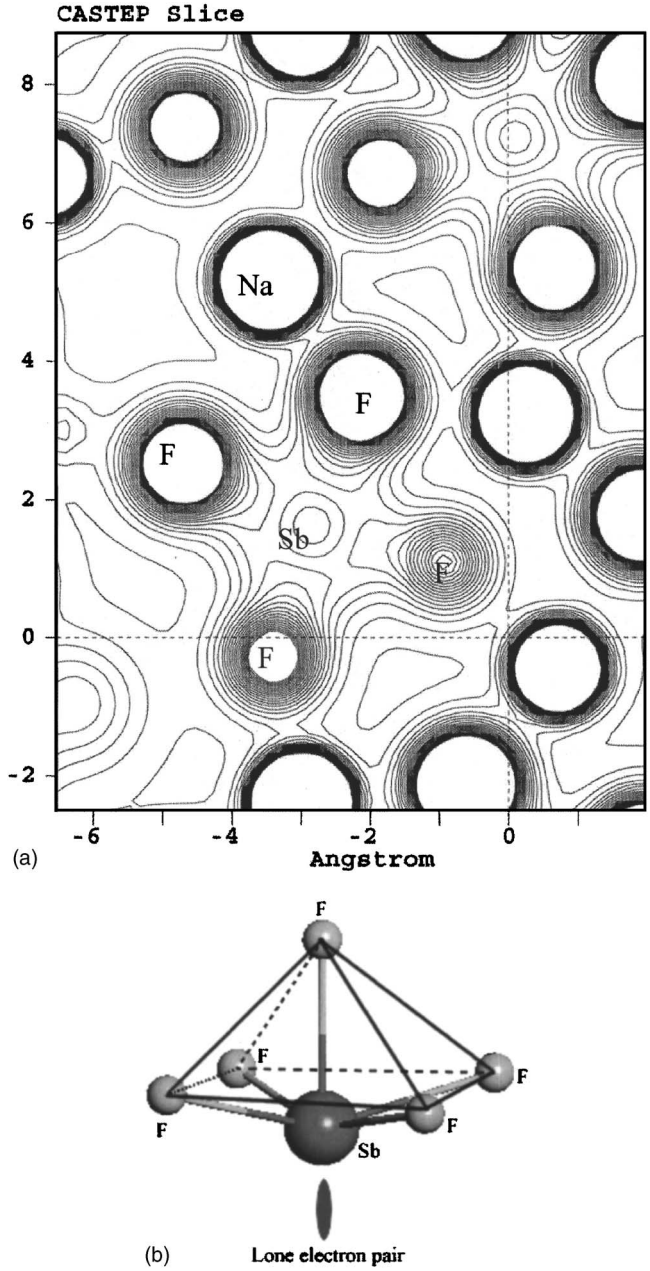

FIG. 4. Charge-density contour map (a) and molecular configurations (b) of Na_2SbF_5.

about two-thirds. For the SHG coefficient the contribution from Na ion is about one-fourth and the one from $(SbF_5)^{2-}$ is about three-quarters.

Based on the above calculations several important conclusions can be obtained as follows: (i) Due to the strong ionic bonding and the larger electronegativity of the fluorine [see Figs. 5(a) and 5(b)] in fluoride NLO crystals, the birefringence and nonlinear susceptibilities of the fluoride crystals are all small (usually, the birefringence is about 0.01 and the SHG coefficient is about 0.1 pm/V). So the application of the fluoride crystals in DUV harmonic generation is not ideal. (ii) However, Na_2SbF_5 is an exception. One can see from Fig. 4 that there is a relatively strong covalent bonding [see Fig. 4(a)] and a lone-pair electron [see Fig. 4(b)] in the $(SbF_5)^{2-}$ group. Obviously, according to the anionic group theory[18–20] the structure of the $(SbF_5)^{2-}$ group with lone pair is very favorable for producing a larger microscopic second-order susceptibilities and a larger anisotropy of the linear optical response. To prove the above idea we have calculated the microscopic second-order susceptibilities of the $(SbF_5)^{2-}$ group using the anionic group theory with a GAUSSIAN'92 *ab initio* program[22] and have compared these with the microscopic second-order susceptibilities of the various boron-oxygen groups in Table III. It is obvious from Table III that even bulk SHG coefficients of most fluoride NLO crystals is small to be compared with the borate series NLO crystals but the microscopic second-order susceptibilities of the $(SbF_5)^{2-}$ group are much larger than those of the borate groups, (B_3O_6) group in particular. Unfortunately, the space arrangement of the $(SbF_5)^{2-}$ groups in the Na_2SbF_5 crystal is unfavorable for producing the large overall SHG coefficients: as a result, d_{14} coefficient of the crystal is only -0.123 pm/V (by GAUSSIAN'92) and -0.154 pm/V (by CASTEP). However, large second-order susceptibilities of the $(SbF_5)^{2-}$ group give us a confidence that could be possible in the fluoride series crystals to search for NLO crystals, which have much larger bulk SHG coefficients and also stronger anisotropy of refractive indices.

TABLE II. The atom-cutting analysis for the Na_2SbF_5 crystal.

	Na+	$(SbF_5)^{2-}$	Sum	Na_2SbF_5
n_x	1.153	1.513		1.566
n_y	1.161	1.510		1.573
n_z	1.169	1.542		1.510
$\Delta n(n_{max}-n_{min})$	0.016	0.031	0.047	0.059
d_{123}(pm/v)	-0.057	-0.161	-0.218	-0.154

IV. CONCLUSION

Ab initio electron band-structure calculations have been carried out using the CASTEP package and the anionic group theory with the GAUSSIAN'92 program to study the optical properties of fluoride crystals. Our investigations are summarized as follows.

(i) The electronic energy-band structures of three fluoride crystals with relatively large band gaps have been obtained. The DOS and PDOS figures reveal the composition of each energy band, and the electron-density contour maps clearly show that the crystals possess a relatively greater ionic bond component but weaker covalent bond. These structural factors result in too small birefringence and overall SHG coefficients. As a result, these fluoride crystals are of limited use in NLO applications.

(ii) However, Na_2SbF_5 is an exceptional crystal consisting of the basic structural unit of the square pyramidal group $(SbF_5)^{2-}$ with a lone-pair electron. The calculations indicate that the structure of this anionic group $(SbF_5)^{2-}$ is favorable for producing a much larger second-order microscopic susceptibility compared with boron-oxygen anion groups, the (B_3O_6) group in

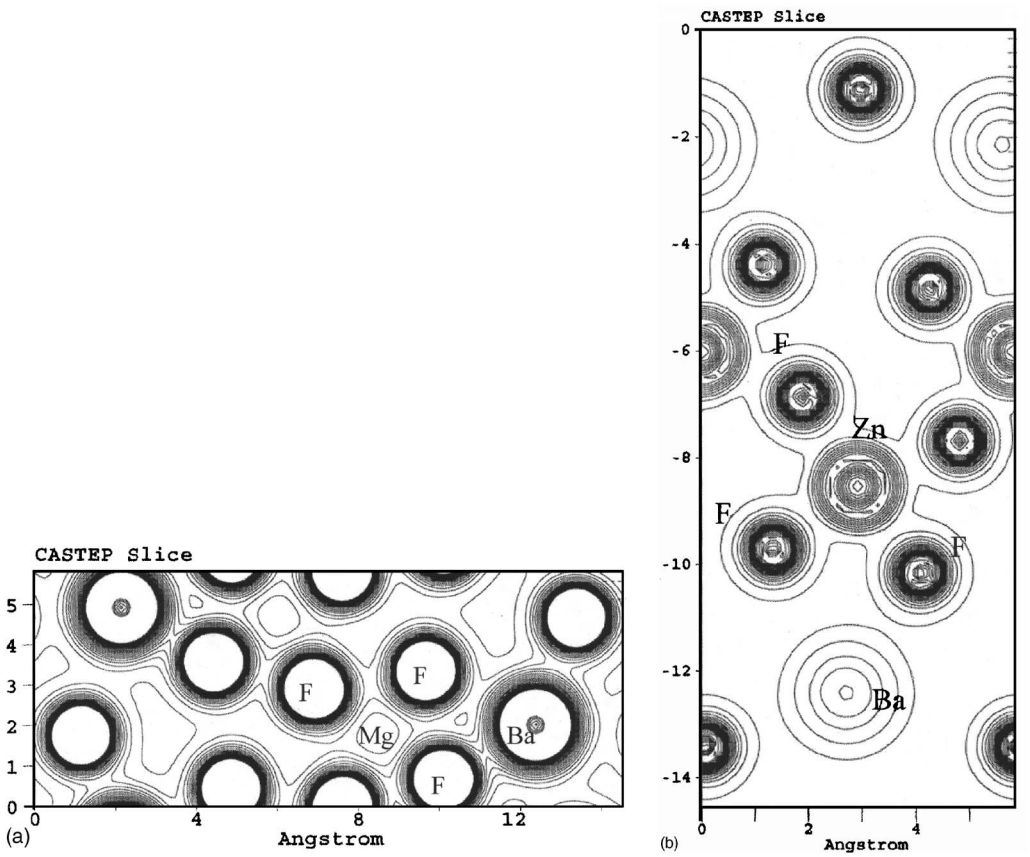

FIG. 5. Charge-density contour map of (a) $BaMgF_4$ and (b) $BaZnF_4$.

particular. However, the spatial arrangement of the $(SbF_5)^{2-}$ group in the Na_2SbF_5 crystal with $P_{2_12_12_1}$ space symmetry is unfavorable for producing large overall SHG coefficients. As a result, d_{14} of the crystal is only −0.123 pm/V (by GAUSSIAN'92) and −0.154 pm/V (by CASTEP). Hence the only approach to search fluoride crystals with large birefringence and NLO coefficients is to identify the fluoride groups with a lone-pair electron and to look further for a favorable spatial arrangement of the fluoride groups.

TABLE III. Calculated values of the microscopic second-order susceptibility of the $(SbF_5)^{2-}$ group and some boron-oxygen groups (Ref. 21) (10^{-31} esu; $\lambda = 1.064\ \mu$m).

Group	Microscopic susceptibility	GAUSSIAN'92
$(SbF_5)^{2-}$	$\chi^{(2)}_{111}$	-6.2729
	$\chi^{(2)}_{222}$	2.1194
	$\chi^{(2)}_{112}$	1.9451
$(BO_3)^{3-}$	$\chi^{(2)}_{111}$	0.4715
	$\chi^{(2)}_{122}$	-0.4715
$(B_3O_6)^{3-}$	$\chi^{(2)}_{111}$	1.55970
	$\chi^{(2)}_{122}$	-1.5520
$(B_3O_7)^{5-}$	$\chi^{(2)}_{111}$	-1.8593
	$\chi^{(2)}_{122}$	0.7618
	$\chi^{(2)}_{133}$	-0.4142
$(BO_4)^{5-}$	$\chi^{(2)}_{123}$	-0.1404
	$\chi^{(2)}_{113}$	0.0055
	$\chi^{(2)}_{223}$	-0.0139

ACKNOWLEDGMENTS

This work is supported by the Chinese National Basic Research Project No. 2004CB619001, NSF 90203016, and M.H.L. is grateful for the support from NSC 89-211-M-032-026. The work is also supported by Supercomputing Center, CNIC, CAS.

[1] M. C. Payne, M. P. Teter, D. C. Allan, T. A. Arias, and J. D. Joannopoulos, Rev. Mod. Phys. **64**, 1045 (1992).
[2] M. D. Segall, P. J. D. Lindan, M. J. Probert, C. J. Pickard, P. J. Hasnip, S. J. Clark, and M. C. Payne, J. Phys.: Condens. Matter **14**, 2717 (2002).
[3] R. G. Parr and W. T. Yang, *Density Functional Theory of Atom-Molecules* (Oxford University Press, Oxford, 1989).
[4] J. Lin, M. H. Lee, Z. P. Liu, C. T. Chen, and C. J. Pickard, Phys. Rev. B **60**, 13380 (1999).
[5] Z. S. Lin, Z. Z. Wang, C. T., Chen, and M. H. Lee, Phys. Rev. B **62**, 1757 (2000).
[6] Z. S. Lin, Z. Z. Wang, C. T. Chen, S. K. Chen, and M. H. Lee, Chem. Phys. Lett. **367**, 523 (2002).
[7] Z. S. Lin, Z. Z. Wang, C. T. Chen, S. K. Chen, and M. H. Lee, J. Appl. Phys. **93**, 9717 (2003).
[8] Z. S. Lin, Z. Z. Wang, C. T. Chen, S. K. Chen, and M. H. Lee, J. Chem. Phys. **118**, 2349 (2003).
[9] Z. S. Lin, Z. Z. Wang, H. T. Yang, C. T. Chen, and M. H. Lee, J. Chem. Phys. **117**, 2809 (2002).
[10] L. Kleinman and D. M. Bylander, Phys. Rev. Lett. **4**, 1425 (1982).
[11] A. M. Rappe, K. M. Rabe, E. Kxiras, and J. D. Joannopoulos, Phys. Rev. B **41**, 1227 (1990).
[12] J. S. Lin, A. Qteish, M. C. Payne, and V. Heine, Phys. Rev. B **47**, 4174 (1993).
[13] R. W. Godby, M. Schluter, and L. J. Sham, Phys. Rev. B **37**, 10159 (1988).
[14] C. S. Wang and B. M. Klein, Phys. Rev. B **24**, 3417 (1981).

[15]S. N. Rashkeev, W. R. L. Lambrecht, and B. Segall, Phys. Rev. B **57**, 3905 (1998).
[16]J. G. Bergman and D. S. Chemla, J. Solid State Chem. **23**, 187 (1978).
[17]J. G. Bergman and G. R. Crame, J. Appl. Phys. **46**, 4645 (1975).
[18]C. T. Chen, Acta Phys. Sin. **25**, 146 (1976).
[19]C. T. Chen, Sci. Sin. **22**, 756 (1979).
[20]C. T. Chen, *Development of New NLO Crystals in the Borate Series*, edited by V. S. Letokhov, C. V. Shank, Y. R. Shen, and H. Walther (Harwood, New York, 1993).
[21]Z. S. Lin, J. Lin, Z. Z. Wang *et al.*, J. Phys.: Condens. Matter **13**, R369 (2001).
[22]*Gaussian 92, Revison A*, Pittsburg, PA, 1992.